



ISSN: 2319-5967

ISO 9001:2008 Certified

International Journal of Engineering Science and Innovative Technology (IJESIT)

Volume 2, Issue 4, July 2013

Influence of Cr³⁺ ion substitution on DC and AC electrical properties of zinc ferrite nanoparticles

Rintu Mary Sebastian¹, Sheena Xavier¹, E M Mohammed¹

¹ Research Department of Physics, Maharaja's College, Ernakulam, Kerala, India

Abstract— Chromium substituted zinc ferrite nanoparticles with general formula $ZnCr_xFe_{2-x}O_4$ ($x = 0.0, 0.2, 0.4, 0.6, 0.8, 1.0$) have been synthesized using sol gel auto combustion method. Rietveld refinement analysis of the XRD pattern indicates the formation of single phase cubic spinel structure having space group $Fd3m$ for all the samples. The lattice constant as well as the crystallite size of the sample was found to decrease with increase in chromium concentration. The surface morphology of the samples was studied from the SEM images. The absorption bands in FTIR spectra are found in the expected range of ferrites and this corroborates the spinel structure of the samples. The DC resistivity at room temperature was observed to decrease with increase in chromium content. The investigation on dielectric constant, dielectric loss factor and AC conductivity was carried out in the frequency range 20Hz to 30MHz from room temperature to 523K. AC conductivity is found to increase with frequency and suggests conduction due to small polaron hopping. Frequency dependence of dielectric constants shows normal behavior and agrees with Koops phenomenological theory of dielectric dispersion. Thermally enhanced drift mobility of charge carriers attributed to the increase in dielectric constant with temperature. The low value of dielectric loss at high frequencies makes Zn – Cr ferrite desirable for high frequency applications.

Index Terms— Dielectric properties, Nanocrystalline materials, Zinc ferrite, Rietveld refinement.

I. INTRODUCTION

Nano sized ferrite with narrow size distribution and uniform particle size are of current research interest due to their broad application in technological fields like targeted drug delivery, medical imaging, electronic devices, magnetic storage devices etc. [1] - [4]. The chemical composition, method of preparation, nature of ions and their site preference among tetrahedral and octahedral sites in lattice influence the structural and electrical properties of spinel ferrites. Among the different spinel ferrites, zinc ferrite is one of the most versatile, due to their wide range of potential applications like as absorbent material, photo catalyst and gas sensors [5], [6].

Sol gel is an attractive preparation method for ferrites due to its good stoichiometric control and production of ultra-fine particles in nano range at relatively low temperature [7]. The incorporation of metal ions to the spinel structure can considerably change the magnetic and electrical properties. Antiferromagnetic nanocrystallites of $ZnFe_2O_4$ and $ZnCr_2O_4$ have been extensively studied [8], [9]. However the structural and electrical properties of Cr³⁺ substituted zinc ferrite has not been investigated in detail. In the present study, the effect of Cr³⁺ substitution on structural and electrical properties of nano crystalline zinc ferrite prepared by sol gel technique is reported..

II. EXPERIMENT

A. Synthesis

Ferrite Sample with chemical formula $ZnCr_xFe_{2-x}O_4$ ($x = 0.0, 0.2, 0.4, 0.6, 0.8, 1.0$) were prepared by simple sol-gel technique. AR grade of zinc nitrate, chromium nitrate, ferric nitrate in the Stoichiometric ratio were used as chemical precursors in ethylene glycol as the solvent. The sol was heated at 60°C until a wet gel of metal nitrates was obtained. The gel was dried at 120°C, which self-ignites to form a fluffy product by the redox reaction of the gel where ethylene glycol acts as the reducing agent and the nitrate ions acts as the oxidant. The obtained powder was ground well and sintered at 400°C for 2 hrs. For dielectric measurements, cylindrical disc shaped pellets of diameter 13 mm and height 1 – 2 mm were made using a hydraulic press by applying a uniform pressure of 5 tons.

B. Characterization

The structural characterization of the prepared samples were done using the X ray diffraction (XRD) patterns recorded using BRUKER make AXS D8 ADVANCE powder X ray Diffract meter with Cu – K α radiation ($\lambda = 1.5406 \text{ \AA}$) at 40 kV and 35 mA from 20° to 80° in steps of 0.02° per second. The Fourier Transform Infrared



ISSN: 2319-5967

ISO 9001:2008 Certified

International Journal of Engineering Science and Innovative Technology (IJESIT)

Volume 2, Issue 4, July 2013

(FTIR) absorption spectra of the prepared sample were recorded using FTIR spectrometer [Thermo Nicolet, Avatar 370] in the wave number range 4000 cm^{-1} to 400 cm^{-1} with potassium bromide (KBr) as binder. Morphological analysis of the zinc ferrite samples were performed by Transmission Electron Microscope (Hitachi Japan H7650). Dielectric measurements were carried out using precision impedance analyzer Wayne Kerr 6500B in the frequency range (20 Hz to 5 MHz) at 300 K. The two faces of the pellet are coated with silver paste to form a parallel plate capacitor with zinc ferrite as the dielectric material. The capacitance of the parallel plate capacitor is given by,

$$C = \frac{\epsilon_0 \epsilon' A}{d} \quad (1)$$

Where A is the area, d the thickness of the pellet, ϵ_0 is the permittivity of free space and ϵ' is the permittivity of the dielectric material. Thus real part of dielectric constant of the sample can be calculated from the relation,

$$\epsilon' = \frac{Cd}{\epsilon_0 A} \quad (2)$$

From the values of real part of dielectric constant and loss tangent the dielectric loss factor (imaginary part of dielectric constant) and AC conductivity of the sample can be calculated using the equation (3) and (4),

$$\epsilon'' = \epsilon' \tan \delta \quad (3)$$

Where $\tan \delta$ is the dielectric loss factor, the energy dissipated in the form of heat when field is applied to the sample

$$\sigma_{AC} = 2\pi f \epsilon_0 \tan \delta \quad (4)$$

The DC resistivity of the samples was recorded at room temperature using an electrometer (KEITHLY 6221 DC and AC current source and 2182 A nanovoltmeter) in two probe methods. Current source applies constant current on sample pellets and voltage developed is measured using the nanovoltmeter. Silver paste was employed for better electrical contact. The electrometer was programmed to get the average resistance R of the pellet by repeating the measurement for different steady current. The resistivity of the ferrite samples is evaluated using the formula,

$$\rho = \frac{RA}{d} \quad (5)$$

Where A, d are the area and thickness of the pellet respectively,

The XRD pattern of all the samples were refined using the GSAS program [10] developed by Larson and Van Dreele, from X – ray powder diffraction data. The space group and initial structural parameters for all the samples were taken as: Fd3m and Wycokoff positions of metal and iron atoms as (0.125, 0.125, 0.125) and (0.5, 0.5, 0.5) respectively and Oxygen in (x, x, x) special position, were $x = 0.2555$. All the octahedral, tetrahedral and oxygen sites were assumed to be fully occupied. Multi term Simpson's rule integration of the Pseudo – Voigt function was used to model the diffraction profiles. The fitting quality of the experimental data is assessed using the following parameters : the goodness of fit (χ^2) which must tend to 1 and two reliability factors R_p and R_{wp} (Weighted difference between measured and calculated values), which must be close to or less than 10% [11].

III. RESULT AND DISCUSSION

A. Structural analysis

XRD pattern of $\text{ZnCr}_x\text{Fe}_{2-x}\text{O}_4$ ($x = 0.0, 0.2, 0.4, 0.6, 0.8, 1.0$) nanoparticles is depicted in Fig. 1. The patterns were compared with standard data (JCPDS card No: 82 – 1042).

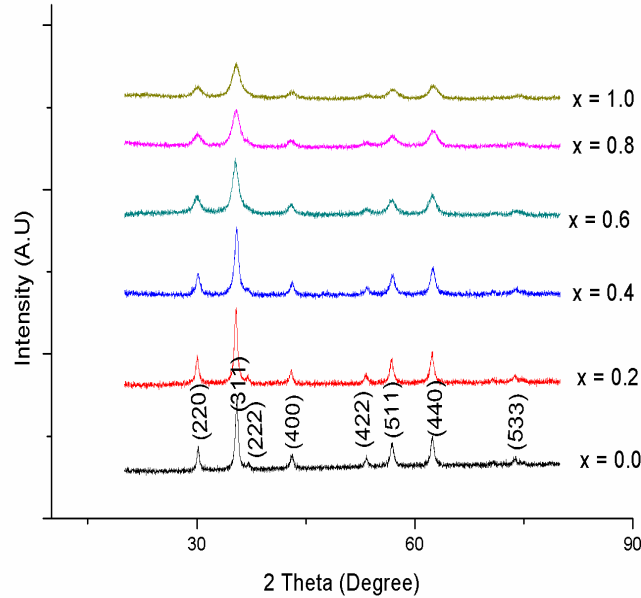
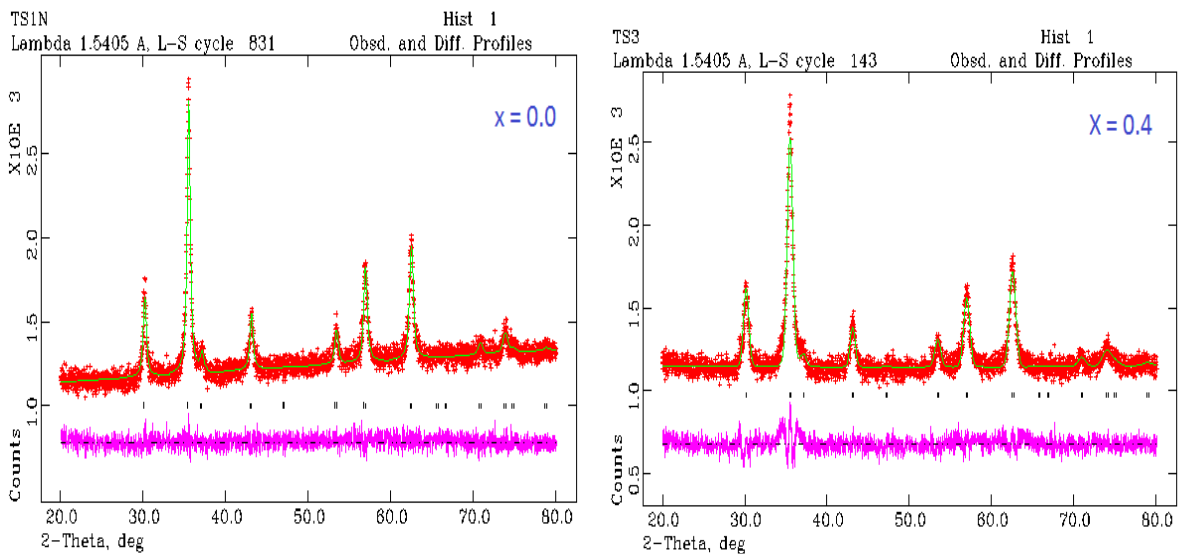


Fig 1: XRD pattern of $ZnCr_xFe_{2-x}O_4$ nanoparticles ($x = 0.0, 0.2, 0.4, 0.6, 0.8, 1.0$)

The crystallite size of all the samples was calculated using the Scherrer formula [12]

$$D = \frac{0.9\lambda}{\beta \cos\theta} \tag{6}$$

Where λ is the X- ray wavelength of the Cu $K\alpha$ radiation ($\lambda = 1.5406 \text{ \AA}$). The angle θ for maximum intensity and full width at half maximum (FWHM or β) were determined by fitting the peaks with Gaussian curve. Rietveld refinement pattern for the samples is represented in Figure 2. X – Ray data points are shown by plus marks; the solid line is the best fit to the data and the tic marks show the positions for the allowed reflections. The lower curve represents the difference between the observed and calculated profiles.



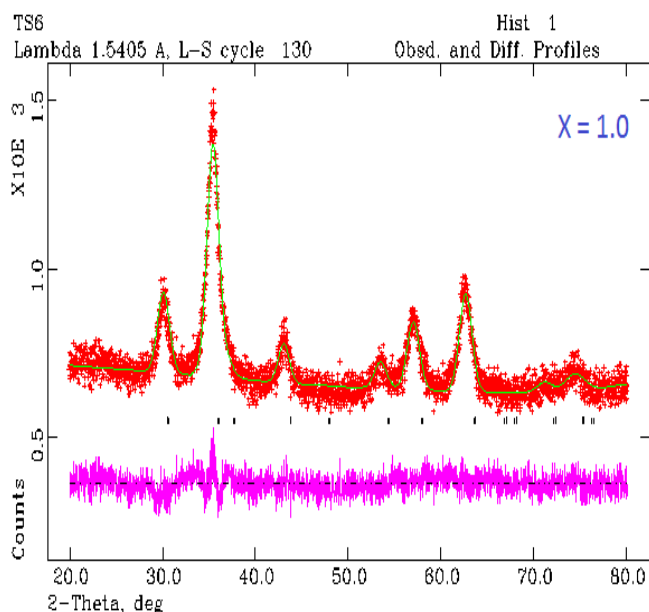


Fig 2 : Rietveld refinement pattern for $ZnCr_xFe_{2-x}O_4$ nanoparticles ($x = 0.0, 0.4, \text{ and } 1.0$)

The values of goodness of fit (χ^2), reliability factors (R_p and R_{wp}), and the lattice constant calculated from Rietveld method are listed in Table 2. The low values of χ^2 , R_p and R_{wp} confirms the goodness of refinement.

Table 1: Rietveld and structural parameters for all the compositions

Parameter	X = 0.0	X = 0.2	X = 0.4	X = 0.6	X = 0.8	X = 1.0
R_p (%)	2.85	2.70	2.70	2.83	3.13	3.36
R_{wp} (%)	2.29	3.40	3.43	3.62	3.92	4.21
χ^2	1.049	1.505	1.414	1.483	1.347	1.262
Lattice Constant (Å)	8.433	8.427	8.410	8.331	8.325	8.282
Unit Cell Volume (Å ³)	599.717	598.438	594.823	578.218	576.969	576.938
Crystallite Size (nm)	18.64 ± 0.3	16.69 ± 0.2	12.90 ± 0.1	8.25 ± 0.1	6.67 ± 0.1	6.13 ± 0.1

From Table 1 it is clear that the lattice constant decreases with increase in chromium content. This decrease in lattice constant with Cr^{3+} content can be explained on the basis of the difference in ionic radii of Fe^{3+} (0.67 Å) and Cr^{3+} (0.64 Å). The replacement of Fe^{3+} with Cr^{3+} leads to shrinkage of the lattice leading to continuous decrease of lattice constant.

B. FTIR Spectra

FTIR spectra of the investigated samples are shown in Fig. 3. The two main absorption bands in the range (600 – 550) cm^{-1} and (450 – 385) cm^{-1} , the typical bands of spinel structure are attributed to the stretching vibrations of the unit cell of the spinel in the tetrahedral (A) site and the metal oxygen vibration in the octahedral (B) site [13].

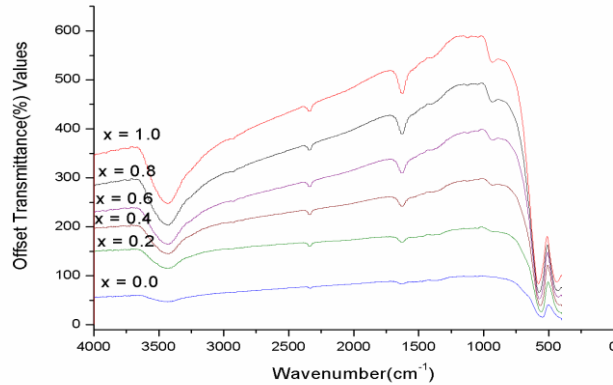


Fig 3: FTIR spectra of $ZnCr_xFe_{2-x}O_4$ series

From Fig. 3 it is clear that Cr^{3+} ion doping, the absorption band ν_2 broadens and shift to the higher frequency side which indicates that Cr^{3+} ions occupy the octahedral site. It can also be noted that as the band broadens and intensity decreases which can be explained on the basis that more disorder states give broader and less intense bands in IR spectra [14]. The bands around $3400cm^{-1}$ and $1600cm^{-1}$ are the contribution of the stretching vibration of free and absorbed water.

C. Scanning Electron Microscopy (SEM)

The surface morphology of the presently investigated ferrite samples were analyzed using SEM micro photographs. Fig. 4 shows the representative SEM photographs of zinc chromium mixed ferrite ($x = 0.0, 0.4, 1.0$). From the photographs it is clear that the grain size decreases with chromium content.

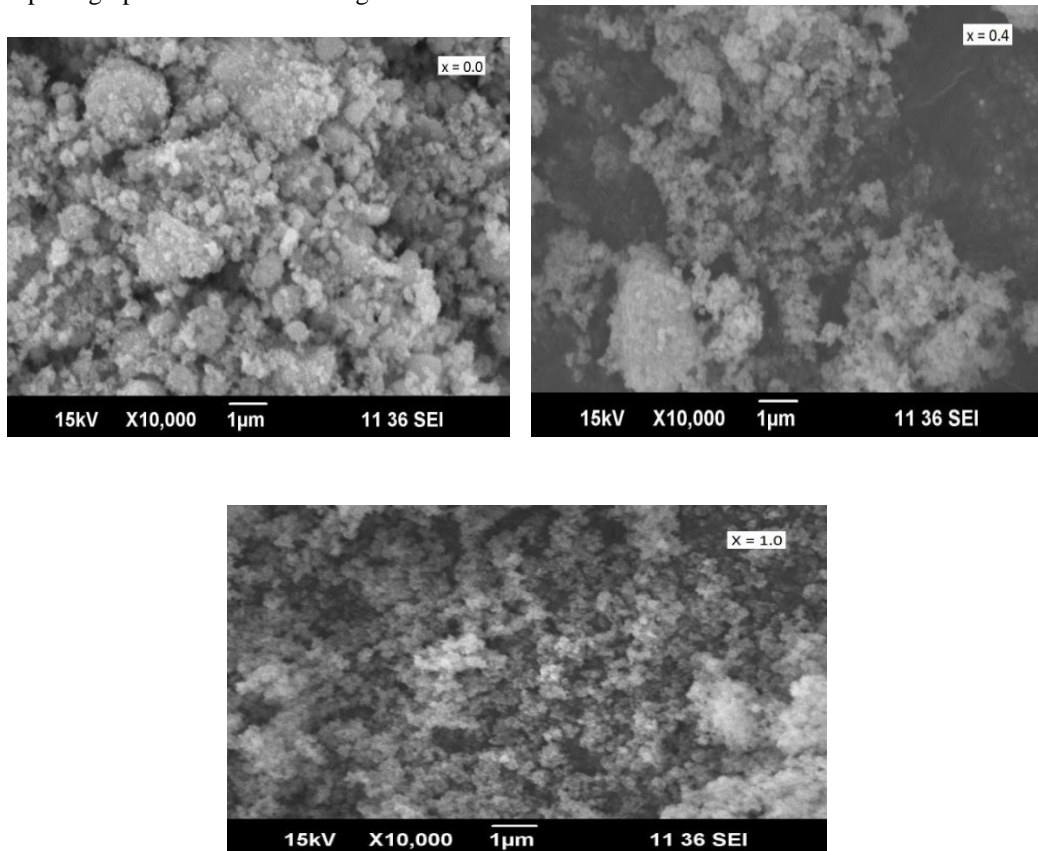


Fig 4: SEM photographs of $ZnCr_xFe_{2-x}O_4$ nano particles ($x = 0.0, 0.4, 1.0$)

A. Electrical Properties

D.1. DC Resistivity

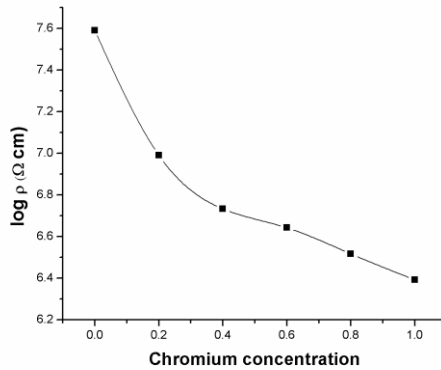


Fig 5: DC resistivity variation with doping concentration at room temperature

The variation of DC resistivity at 300K with chromium doping concentration is shown in Fig. 5. It is observed that the resistivity of the samples decreases with Cr³⁺ content. The conduction in ferrite occurs mainly due to the hopping of electrons between ions of the same element existing in different valancies in equivalent lattice sites [15]. It is reported that Zn²⁺ ions prefer the tetrahedral (A) sites; Cr³⁺ prefer the occupation of octahedral (B) sites [16]. While Fe³⁺ ions partially occupy the A and B sites. The continuous decrease of resistivity with chromium content may be due to the increasing presence of chromium ion on the octahedral sites, which is clearly seen from the FTIR spectrum.

D.2. DC Resistivity

Variation of real part of dielectric constant and imaginary part of dielectric constant with frequency at 300K is depicted in Fig. 6 and Fig. 7. Imaginary part of dielectric constant is also known as dielectric loss factor and is a measure of energy loss within the dielectric medium.

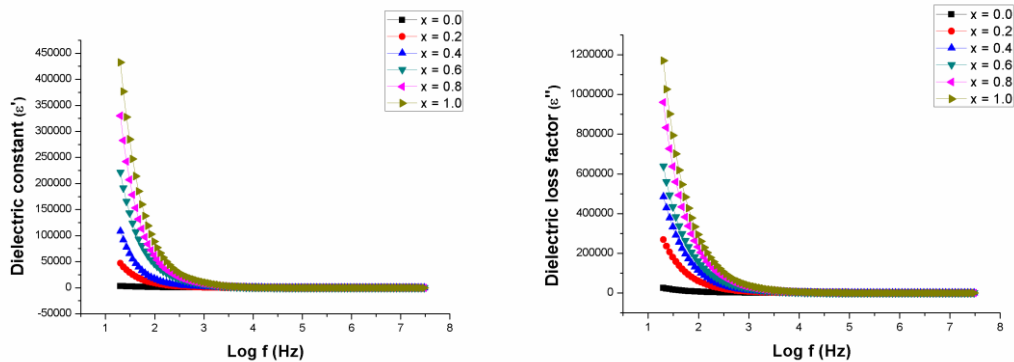


Fig 6 & Fig 7: Frequency variation of dielectric constant and dielectric loss factor

It can be clearly seen that both real and imaginary part of dielectric exhibits an inverse dependence on frequency. The decrease in both real and imaginary part of dielectric constant is sharp at the lower frequency region and remains almost a constant at high frequencies. The rapid decrease of permittivity in the low frequency range can be explained by the basic Koop's phenomenological theory [17], which considers the dielectric structure as an inhomogeneous medium of Maxwell-Wagner type [18]. In this model, the dielectric structure of ferrites is assumed to be consisting of highly conducting grains, separated by poorly conducting boundaries. It is known that the grain boundaries are more effective at low frequencies and the grain at high frequencies [19]. During the electron hopping process between Fe²⁺ to Fe³⁺, the high resistance of the grain boundaries makes the electrons accumulate on the grain boundaries, producing space charge polarization, resulting in comparatively high value of dielectric constant at low frequencies, But as frequency increases the grains come into action reducing the dielectric constant

rapidly due to decrease in space charge polarization. Even if the conductivity increases with frequency the hopping of electrons cannot follow the applied frequency of the alternating field, consequently the dielectric constants attains a constant value at higher frequencies. It is evident from the figure that both real and imaginary part of dielectric constant increases with Cr^{3+} ion doping. It should be noted that the dielectric constant is higher for Cr^{3+} substituted zinc ferrite than zinc ferrite. Similar result has been reported for Nd^{3+} substituted zinc ferrite [20]. The electron exchange between $\text{Fe}^{2+} \leftrightarrow \text{Fe}^{3+}$ ion pairs determines the dielectric polarization and whose magnitude depends on the percentage of Fe^{2+} and Fe^{3+} ion pairs at A and B sites. The increase in dielectric constants (ϵ' and ϵ'') in the present case can be explained by low concentration of Fe^{2+} ion at the B site leading to low value of resistivity, hence high value of dielectric parameter [21].

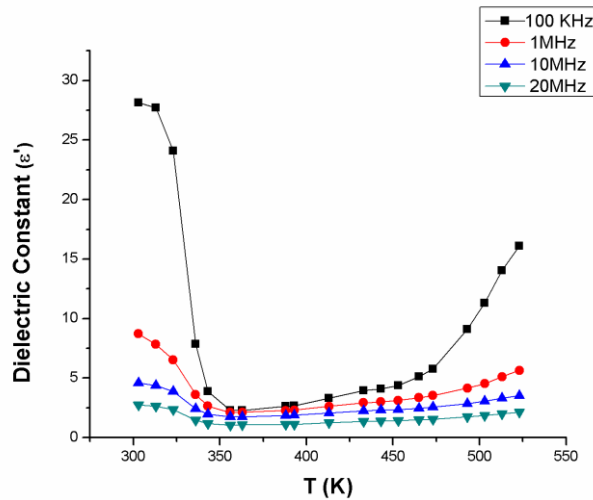


Fig 8: Variation of Dielectric constant temperature for the sample with $x = 0.4$

Temperature dependence of dielectric constant for the sample $\text{ZnCr}_{0.4}\text{Fe}_{1.6}\text{O}_4$ at four different frequencies is depicted in Fig. 8. All the other compositions showed similar behaviour except the pure zinc ferrite sample which does not exhibit the initial decrease in dielectric constant. Dielectric constant in ferrites is mainly due to interfacial, dipolar, atomic and electronic types of polarization. At low frequencies, contribution of dipolar and interfacial polarization dominates and both of these polarizations are temperature dependent [15]. This explains the rapid variation in dielectric constant with temperature at low frequencies. But a relatively insignificant variation of dielectric constant with temperature is observed at high frequencies, as the temperature dependence of electronic and ionic polarizations which dominates at high frequencies, is insignificant. The initial decrease in ϵ' , which is absent in pure sample, indicates the metallic nature of the samples in the lower temperature region as a result of chromium substitution [22]. The dielectric constant increases with temperature due to the increase in drift mobility of charge carries. Hopping of electrons is thermally activated by increase in temperature, resulting in an increase in space charge polarization and thus dielectric constant increases with temperature [19], [23].

D.3. AC Conductivity

The frequency variation of AC conductivity at room temperature for zinc chromium mixed ferrite is depicted in Fig. 9.

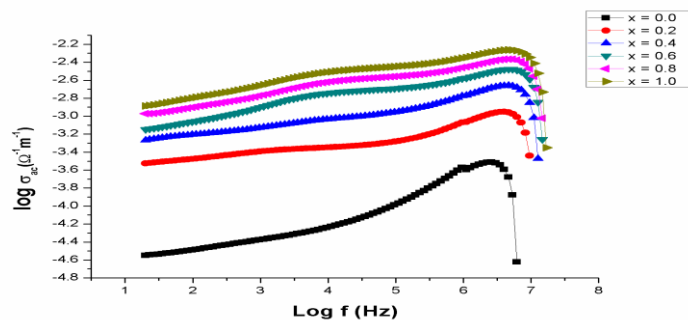


Fig 9: Variation of AC conductivity with frequency



ISSN: 2319-5967

ISO 9001:2008 Certified

International Journal of Engineering Science and Innovative Technology (IJESIT)

Volume 2, Issue 4, July 2013

The increase in AC conductivity with frequency for all the compositions can be explained using Maxwell Wagner two layer model of polycrystalline ferrite [24]. At low frequency the poorly conducting grain boundaries are more prominent hence leading to low value of conductivity. But as frequency increases, conductive grains become active, which results in increase of conduction. The plots of all the Zn – Cr ferrite samples are almost linear, which points to conduction due to small polaron hopping [25]. The AC conductivity is found to increase with chromium ion concentration. The AC conductivity is first observed to increase with frequency and reaches a maximum value and then decreases. As the frequency of the applied field increases, the hopping of charge carriers also increases thereby increasing the conductivity. But at higher frequencies, the hopping of charge carriers could not follow the applied field resulting in decrease in the ac conductivity values. Similar results were reported by other authors also [22], [26].

IV. CONCLUSION

Nano particles of $ZnCr_xFe_{2-x}O_4$ ($x = 0.0, 0.2, 0.4, 0.6, 0.8, 1.0$) mixed ferrite were synthesized by the sol – gel technique. All the studied samples were pure cubic spinel type ferrite without any impurity phase. The lattice constant of all the samples calculated from Rietveld analysis suggests the contraction of the unit cell with chromium doping. Chromium doping resulted in a decrease in particle size in Zn – Cr ferrite. The absorption bands in FTIR spectra are found in the expected range of ferrites and this corroborates the spinel structure of the samples. The absorption bands ν_2 broadens and shifts to the higher frequency side which indicates the substitution of Fe^{3+} ions on octahedral sites by Cr^{3+} ions. Frequency dependence of dielectric constant shows normal behavior and agrees well with Koop's theory. Thermally enhanced drift mobility of charge carriers attributed to the increase in dielectric constant with temperature. AC conductivity increases with frequency in all the samples. Low value of dielectric loss at high frequencies makes nano sized chromium doped zinc ferrite particularly useful in high frequency devices as well as power application devices.

REFERENCES

- [1] W. C. Kim, S. J. Kim, S. W. Lee and C.S. Kim, "Growth of ultrafine NiCuZn ferrite and magnetic property by solgel method", *J. Magn. Magn. Mater.*, 226, 1418 – 20, 2001.
- [2] M. Mozaffari, S. Manouchehri, M.H. Yousefi and J. Amighian, "The effect of solution temperature on crystallite size and magnetic properties of Zn substituted Co ferrite nanoparticles", *J. Magn. Magn. Mater.*, 322, 383 – 388, 2010.
- [3] Lucas W Yeary, Ji Won Moon, Claudia Rawn, Lonnie J Lane, Adam Rondinone, James R Tompson, Bryan C Chakoumakis and Tomy J Phelps, "Magnetic properties of bio synthesized zinc ferrite nanoparticles", *J. Magn. Magn. Mater.*, 323, 3043 – 3048, 2011.
- [4] Mohd. Hashim, Alimuddin, Shalendra Kumar, B.H. Koo, Sagar E. Shirsath, E.M Mohammed, Jyoti Shah, R.K. Kotnala, H.K. Choi, H. Choi, H. Chung and Ravi Kumar , " Structural, electrical and magnetic properties of Co – Cu ferrite nano particles", *J. Alloys Compd.* 518 11- 18, 2012.
- [5] Ping Hu, De – an Pan, Xim Feng Wang, Shen – Gen Zhag and Alex A Volinsky,"Fuel additives and heat treatment effect on nanocrystalline zinc ferrite phase composition", *J Magn. Magn. Mater.* 323, 569 – 573, 2011.
- [6] Yan Xu, Yantian Liang, Lijuan Jiang, Huarui Wu, Hongzhi Zhao and Desheng Xui,"Preparation and magnetic properties of $ZnFe_2O_4$ nanotubes", *J. Nanomaterials.* 10, 525967, 5 pages, 2011.
- [7] M. Srivastava, Chaubey S and Ojha A.K, "Investigation on size dependent structural and magnetic behavior of nickel ferrite nanoparticles prepared by Sol – Gel and hydrothermal method", *Mater. Chem. Phys.* 118, 174 – 180, 2009.
- [8] X.H. Chen, H.T. Zhang, C.H Wang, X.G. Luo and P.H. Li, "Effect of particle size on magnetic properties of zinc chromite synthesized by sol- gel method", *J. Appl. Phys. Lett* 81, 4419, 2002.
- [9] L.D. Tung, V Kolesnichenko, G. Caruntu, D. Caruntu, Y. Remond, V.O. Golub, C.J.O. Connor and L. Spinu, *J. Physica B: Condensed Matter* 319, 116 – 121, 2002.
- [10] Larson C and R B Van Dreele, 2001, <ftp://ftp.lanl.gov/public/gsas>
- [11] J.A. Gomes, M.H. Sousa, F.A Tourinbo, J Mestnik Filho, R Itri and J. Depeyrot,"Rietveld structure refinement of the cation distribution in ferrite fine particles studied by X ray powder diffraction", *J Magn. Magn. Mater.*289, 184 – 187, 2005.
- [12] Lawrence Kumar, Pawan Kumar, Amarendra and Manoranjan Kar, "Rietveld analysis of XRD patterns of different sizes of nanocrystalline cobalt ferrite", *International Nano letters* 3:8, 2013.



ISSN: 2319-5967

ISO 9001:2008 Certified

International Journal of Engineering Science and Innovative Technology (IJESIT)

Volume 2, Issue 4, July 2013

- [13] R.D. Waldron “Infrared Spectroscopy of Ferrites” Phys. Rev. 99, 1727, 1955.
- [14] A.B. Gadkari, T.J Shinde and P.N. Vasambekar, “Structural analysis of Y^{3+} doped Mg – Cd ferrites prepared by oxalate co – precipitation method” Mater. Chem. Phys. 114, 505 – 510, 2009.
- [15] V. Verma, O.P. Thakur, C. Prakash, T.G God and R.C Mendiratta, “Temperature dependence of electrical properties of nickel – zinc ferrite processed by the citrate precursor technique”, Mater. Sci. Eng. B, 116,1-6. 2005.
- [16] S.M. Patange, Sagar E Shirsath, B.G Toksha, S.S Jadhav, S.J Shukla and K.M. Jadhav, “Cation distribution by rietveld, spectral and magnetic studies of chromium substituted nickel ferrites”, J. Appl. Phys A 95, 429 – 434,2009.
- [17] Koop C G, “On the dispersion of resistivity and dielectric constant of some semiconductors at audio frequency”, Phys. Rev. 83, 121- 124, 1951.
- [18] E Veena Gopalan, K.A. Malini, S. Saravanan, D. Sakthi Kumar, Yasuhiko Yoshida and M.R. Anatharaman, “Evidence for polaron conduction in nano structured manganese ferrite”, J. Phys. D: Appl. Phys. 41, 185005(9pp), 2008.
- [19] Binu P Jacob, Smitha Thankachen, Sheena Xavier and E.M. Mohammed, “Dielectric behavior and AC conductivity of Tb^{3+} doped $Ni_{0.4}Zn_{0.6}Fe_2O_4$ nanoparticles”, J. Alloys Compd.541, 29 – 35,2012.
- [20] T.J. Shinde, A.B. Gadkari and P.N. Vasambekar, “Effect of Nd^{3+} substitution on structural and electrical properties of nanocrystalline zinc ferrite”, J Magn. Magn. Mater. 322, 2777- 2781, 2010.
- [21] Erum Pervaiz and I H Gul, “Structural and magnetic studies of Gd^{3+} doped cobalt ferrite nanoparticles”, International Journal of Current Engineering and Technology, ISSN 22777 – 4106, Vol. 2, No.4, Dec 2012.
- [22] Binu P Jacob, Smitha Thankachen, Sheena Xavier and E.M. Mohammed, “Effect of Tb^{3+} substitution on structural, electrical and magnetic properties of sol – gel synthesized nanocrystalline nickel ferrite”, J. Alloys Compd.578, 314 – 319, 2013.
- [23] M.A Ahamed and N. Okasha, “Role of Cu^{2+} concentration on the structural and transport properties of Cr – Zn ferrite”, J. Magn.Magn. Mater. 321, 3436- 3441, 2009.
- [24] Mathew George, Swapna S Nair, K.A. Malini, P.A. Joy and M.R. Anatharaman, “Finite size effect on the electrical properties of sol – gel synthesis of $CoFe_2O_4$ powder; derived from Maxwell Wagner theory and evidence of surface polarization effect”, J. Phys. D: Appl. Phys. 40, 1593–1602, 2007.
- [25] R.S. Devan and B.K. Chougule, “Effect of composition on coupled electric, magnetic and dielectric properties of two phase particulate magneto electric composite”, J. Appl. Phys. 101, 014109(6 pages), 2007.
- [26] E. Veena Gopalan, P.A Joy, I.A. Al – Omari, D. Sakthi Kumar, Yasuhiko Yoshida, M.R. Anatharaman, “On the structural and electrical properties of sol – gel derived nanosized cobalt ferrite”, J. Alloys Compd.485, 711 – 717, 2009.